Development, Growth & Differentiation
The Japanese Society of Developmental Biologists
Develop. Growth Differ. (2015) **57**, 369–377 doi: 10.1111/dgd.12216

Original Article

A transportable, inexpensive electroporator for *in utero* electroporation

Torsten Bullmann,[1,2,3]* Thomas Arendt,[3] Urs Frey[1] and Carina Hanashima[2]

[1]*Frey Initiative Research Unit, RIKEN Quantitative Biology Center, 2-2-3 Minatojima-minamimachi, Chuo-ku, Kobe 650-0047, Japan;* [2]*Laboratory for Neocortical Development, RIKEN Center for Developmental Biology, 2-2-3 Minatojima-minamimachi, Chuo-ku, Kobe 650-0047, Japan; and* [3]*Department of Molecular and Cellular Mechanisms of Neurodegeneration, Paul Flechsig Institute of Brain Research, University of Leipzig, Liebigstraβe 19, 04103, Leipzig, Germany*

Electroporation is a useful technique to study gene function during development but its broad application is hampered due to the expensive equipment needed. We describe the construction of a transportable, simple and inexpensive electroporator delivering square pulses with varying length and amplitude. The device was successfully used for *in utero* electroporation in mouse with a performance comparable to that of commercial products.

Key words: cortex, electronic circuit, electroporation, hippocampus.

Introduction

Introduction of DNA by electroporation is a useful technique in the field of developmental biology (Muramatsu *et al.* 1997; Saito & Nakatsuji 2001; Fukuchi-Shimogori and Grove, 2001; Tabata & Nakajima 2001; reviews: Taniguchi *et al.* 2012; Nakamura & Funahashi 2013). Introduction of expression plasmids and shRNA can achieve overexpression or knockdown of a target gene without the need to engineer transgenic animals (review: LoTurco *et al.* 2009). It is especially useful in combination with time-lapse imaging (Okamoto *et al.* 2013; review: Nishimura *et al.* 2012). Furthermore it is readily applicable to a wide range of model organisms including chick (*in ovo* electroporation), mice (*in utero* electroporation) and insects (Ando & Fujiwara 2013). In contrast to electroporation of bacteria, which requires short, high voltage pulses (several 100 V, few ms), electroporation of tissue of higher organisms requires more mild conditions. Low voltage (10–50 V), long lasting (20–100 ms) square pulses are delivered four to eight times with a short interval (between 0.5 and 2 s). The precise parameters, and other experimental conditions, including shape and physical arrangement of the electrodes, must be optimized for the specific application.

*Author to whom all correspondence should be addressed.
Email: bullmann.torsten@gmail.com
Received 9 March 2015; revised 31 March 2015; accepted 8 April 2015.

The equipment needed for electroporation includes at least a micropipette puller to prepare the micropipettes for injection of DNA and an electroporator. Unfortunately the cost of commercially available electroporators is rather high (at least $10 000). This motivated us to build a transportable, simple and inexpensive electroporator delivering square pulses with varying length and amplitude. There have been reports of low-cost, handmade electroporators for insects only, and their applicability for vertebrates was not tested. Furthermore, the described devices required computer programs for control of voltage pulses ($200, Ando & Fujiwara 2013) or the pulse length could not be varied ($85, Sugimoto & Tsuchida 2014). There are several different designs for electroporators (Puc *et al.* 2004) but the above technical requirements can already be fulfilled using a relay driven by a simple timer. The circuit described here costs about $50 and can be assembled in <1 day by anyone who has a little experience in soldering. Using batteries as a power source it is also a transportable and safe device, which has been successfully used for *in utero* electroporation in mouse.

Materials and methods

Circuit design and assembly

Most electroporation protocols use a sequence of four to five square pulses at 30–50 V DC lasting 50–100 ms delivered usually with an inter-pulse interval of 1–2 s. The latter interval can be achieved by pressing a trigger several times while counting the seconds.

Therefore the circuit (Fig. 1A) implements only a simple timer triggered by a foot switch and connected to a standard relay that is able to switch on and off in milliseconds the voltage delivered to the tweezers electrodes. This voltage can be provided by a series of batteries.

The timer NE555 is a very popular integrated circuit since its invention by Hans Camenzind in 1971 and can be used to generate single or repeated pulses. Here we use it in the monostable operation mode, where it delivers a single pulse upon trigger. The discharge of capacitor (C_2) through the resistor (R_3) determines the length of the pulse. When the voltage reaches two-thirds of the supply voltage the pulse ends. Therefore, the pulse width can be calculated according to the formula $T_{Pulse} = C_2 \cdot R_3 \cdot \ln(3)$. With a variable resistor of 20 kΩ the maximum pulse can be up to $T_{Pulse} \approx 10\ \mu F \cdot 20\ k\Omega \cdot 1.1 = 220$ ms. The NE555 timer is started by an active low trigger, which means that the voltage at TRIG input must fall below a threshold of one-third of the supply voltage. Furthermore, the voltage must rise above this threshold before the timer ends; otherwise it would retrigger the circuit. Therefore the trigger is connected to a capacitor (C_1), which is connected on both terminals to pull-up resistors (R_1 and R_2). When the foot switch (connected through J_1) or the manual push-button switch (S_1) is pressed, the TRIG input is instantly released. But the capacitor C_1 is quickly charged though R_2. Within $T_{Trig} = C_1 \cdot R_2 \cdot \ln(3/2) \approx 1\ \mu F \cdot 10\ k\Omega \cdot 0.4 = 4$ ms the trigger is again pulled up. Upon release of the foot switch the capacitor is de-charged through R_1+R_2 without triggering a pulse. As a side-effect, this RC circuit also acts as a de-bouncer for the foot switch. A resistor (R_4) connects the output of the NE555 (OUT) to the base of a standard low-power transistor (Q) driving both a relay (K) and an LED (D_1, current limited by R_5). The second diode in reverse polarity (D_2) shunts the reverse voltage generated by the collapse of the magnetic field when voltage is removed from the relay coil. Otherwise this reverse voltage would destroy the transistor (Q). This diode (D_2) can be omitted when the used relay already has a build-in shunting diode.

The LM317 integrated circuit is used as a current limiter, to protect the relay from high load or even short circuit, which otherwise would cause the contacts to stick together. The LM317 is actually an adjustable voltage regulator. If the voltage drop over the resistor (R_6) is exceeding 1.25 V the extra power is wasted as heat. Therefore, the current limit is $I = 1.25\ V/10\ \Omega = 125$ mA. This is much higher as the actual current flowing through the tweezers electrodes during electroporation, which is usually only 50–70 mA even at 50 V. There are different manufacturers for the LM317, and therefore one should carefully check the specifications for the $V_{in} - V_{out}$ difference, which is usually in the range of 3–40 V. Due to the variability in the manufacturing the actual margin is wider and extends to 45 V for most devices. Another possibility is to close the switch S3, which disables the current limiter.

For the relay a miniature latching relay (e.g. Fujitsu FTR-K1CK012W, response time <15 ms) or reed relay (e.g. celduc D81A3108X7, response time <2 ms) can be used. A reed relay is preferred; the encapsulated reed contacts are resistant to corrosion and offering high operating speed, high reliability and long life. On the other hand this type of relay is more susceptible to higher loads (for a typical operating range see insert in Fig. 1A). Depending on the relay used, the switch shows bouncing, which can last up to 2 ms. However, as shown below, this does not affect the electroporation at all. For testing purposes, the push-button switch S_4 can be closed to bypass the relay, e.g. for measuring the voltage of the external power supply (connected at J_2) on the electrodes (through J_3).

The circuit was first assembled on a solderless breadboard (Fig. 1B,C) and tested connecting the output to an extra LED. Afterwards the components were soldered to a printed circuit board (PCB). This is straightforward using a PCB that has the same layout as the breadboard (see Table 1). Finally the electroporator was assembled using a case with all connectors and switches on the front plate (Fig. 1D). We built two versions of the electroporator. The first one used a small case (width × height × depth = 125 × 40 × 74 in mm) and weights only 108 g including battery (Fig. 1E). In the other version the pulse width was fixed by using a fixed resistor for $R_3 = 10$ kΩ and a smaller capacitor $C_2 = 4.7$ pF (pulse length $T_{Pulse} \sim 4.7\ \mu F \cdot 10\ k\Omega \cdot 1.1 = 52$ ms calculated; ~60 ms measured) and a latching relay was used. The case (width × height × depth = 208 × 69 × 190 in mm) also included the variable power supply made of five 9 V battery blocks serially connected with an in-between line to a rotary switch, so that the electroporation voltage could be selected at 9, 18, 27, 36, 45 V using the rotary switch (Fig. 1F). The total weight of this electroporator was 570 g without batteries and could be easily transported from one laboratory to another. After inserting in the batteries the device was ready for stand-alone operation.

Animals

Institute of Cancer Research (ICR) mice were obtained timed-pregnant from the Animal Housing Facility of the RIKEN CDB. The day the vaginal plug was detected

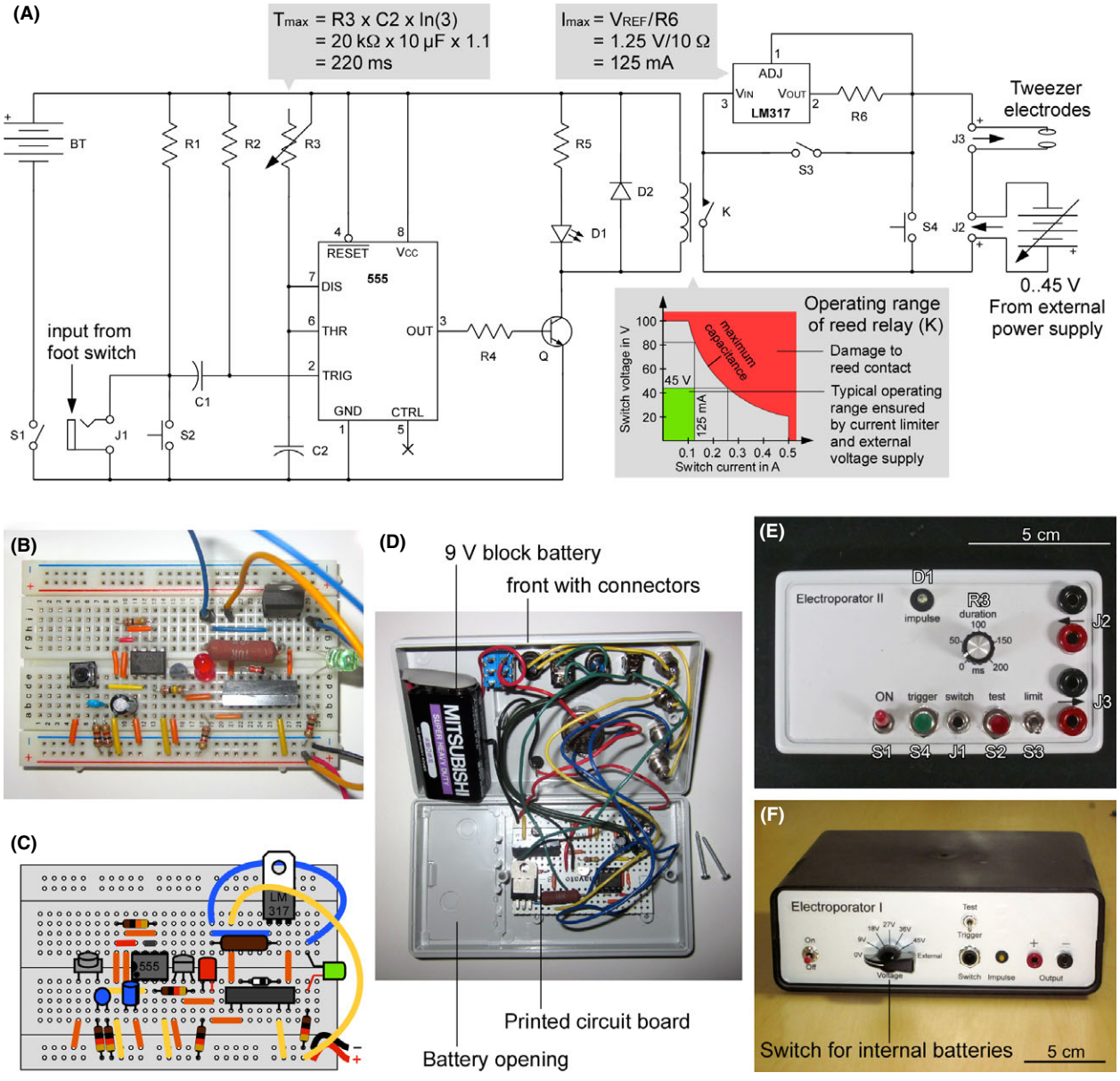

Fig. 1. Electroporator circuit (A). The battery is on the left, followed by the trigger, timer circuit, relay, current limiter, and variable power supply for electroporation; the output to the tweezers' electrodes is shown in the upper right corner. The corresponding parts list can be found in Table 1. Gray boxes above show the calculation of maximum pulse length (220 ms) and current (125 mA). A sketch with the operating range of a typical reed relay is shown in the lower left corner. The circuit was first tested using a solderless bread board (B) before the components were soldered to a breadboard printed circuit board mounted in a plastic case including the power supply for the timer circuit (D). The schematic (C) corresponding to the image of the breadboard shows a pictorial description of the components (Fritzing; http://fritzing.org), including e.g. jumper wires (colored yellow, orange and gray for different lengths), resistors (standard color coded for 10 kΩ, dark brown for 10 Ω) and the miniature-latching relay (dark gray block). The front plate of the final electroporator holds all connectors, switches and the control LED (E). The first version of the electroporator (F) was housed in a slightly bigger case. This case houses a variable power supply for electroporation using five 9 V battery blocks serially connected with an in-between line to a rotary switch, thereby providing 9, 18, 27, 36, 45 V for electroporation.

was designated as E0.5. The Animal Care and Use Committee of RIKEN approved all protocols for animal experiments. Animals of either sex were used in the experiments.

Plasmids for injections

pCAG-enhanced green fluorescent protein (EGFP) and pCAG-DsRed are available from addgene. They were

Table 1. Electronic parts list

Part	Approximate cost
R1 = R2 = R4 = R5 = 10 kΩ resistor	4 × 0.11€
R3 = 20 kΩ potentiometer, linear type	1.58€
R6 = 10 Ω general purpose (e.g. 1/4 W) resistor	0.38€
C1 = 1 μF general purpose (e.g. aluminum) electrolytic capacitor	0.11€
C2 = 10 μF general purpose (e.g. aluminum) electrolytic capacitor	0.11€
IC1 = NE555 timer	0.24€
IC2 = LM317 adjustable voltage regulator	0.98€
BT = 9 V block battery with connectors	3.00€
Q = general purpose low-power NPN type transistor (e.g. KTC3198, 2N3904)	0.16€
K = miniature reed relay (e.g. celduc D81A3108X7, Günther 35701331121) or miniature latching relay (e.g. Fujitsu FTR-K1CK012W)	2.60€ or 1.62€
S1 = toggle switch (red)	0.96€
S2 = S4 = push-button switch	2 × 1.12€
S3 = toggle switch	0.96€
D1 = general purpose low-power LED	0.23€
D2 = general purpose low-power diode (1N4148)	0.04€
J1 = phone jack (e.g. 3.5 mm mono)	1.17€
J2 = J3 = pair of red and black banana jacks	4 × 0.61€
Half-sized breadboard printed circuit board (e.g. Sunhayato, Adafruit)	4.00€
Standard insulated single-strand wire (e.g. 28AWG, 0.08 mm^2 cross section)	1.00€
Plastic case with battery compartment (e.g. Strapubox, 6006)	6.63€
Foot switch with phone connector (e.g. Conrad, FS 50)	10.95€
Sum	40.22€†

†Total cost below $50.

Table 2. Electroporation protocol

Preparation
1. Pull glass capillaries with a long tapper (~1 cm)
2. Prepare pentobarbital working solution:
   900 all sterile physiological saline + 100 μL pentobarbital stock
3. Prepare DNA injection solution
   1 μg/μL plasmid DNA in physiological saline
   0.05% Fast Green
4. Turn on the electroporator† and connect the tweezers electrodes

Surgery
5. Weight and anesthetize the pregnant mouse by intraperitoneal injection:
   Injection volume = 800 μL/40 g body weight
6. Fill glass capillary with DNA injection solution
7. Connect injection capillary to the mouth piece, break tip down to 200 μm diameter and apply gentle pressure: a small drop should form at the tip
8. Put the mouse on the heating pad and disinfect abdominal skin using 70% Ethanol, wipe off
9. Open the abdominal skin 2–3 cm along the midline
10. Put sterile paper tissue over the abdomen with a short slit over the opening and moisture with sterile saline
11. Open the peritoneum along the linea alba
12. Expose the left uterine horn, count the embryos‡
13. Begin with the most distal embryo
14. Hold the embryo between thumb and index finger, careful position the head§
15. Inject DNA solution into the lateral ventricle
16. Electroporation using tweezers-type electrodes
17. Electroporate the other embryos, then place back the left uterine horn and proceed with the right uterine horn¶
18. Suture the peritoneum with Nylon thread
19. Suture the skin with silk thread
20. Keep the mouse warm until recovery from anesthesia

†It is advised to check the batteries using a voltmeter. ‡During the whole procedure the uterus must be kept moist by frequent application of warm physiological saline. §It is important to handle embryos carefully. ¶Surgery should be completed within 30 min.

transformed by heat shock into chemical competent *Escherichia coli*, DH5alpha. Endotoxin-free DNA was prepared from 100 mL cultures in LB medium using a kit (EndoFree Plasmid Maxi Kit; Qiagen). DNA stocks had a final concentration of 10 μg/μL in TE buffer (10 mmol/L Tris/HCl, pH 8.0; 1 mmol/L EDTA) and were stored at −30°C. Fast Green stock was prepared from powder (F7252; Sigma) at 1% w/v in physiological saline (0.90% w/v of NaCl), thoroughly vortexed, sterile filtered and stored at −30°C. Injection solutions containing 1 μg/μL DNA and 0.1% w/v Fast Green were prepared immediately before use.

In utero *electroporation*

Injection capillaries for DNA injections were pulled on a Sutter puller from standard disposable micro hematocrit capillary tubes without heparinization (Roth) and filled with DNA solution using Microloader tips (Eppendorf). *In utero* electroporation (see Table 2) was carried out as described previously (Tabata & Nakajima 2001) with minor modifications (Gonda *et al.* 2013; Okamoto *et al.*, 2013). Briefly, timed-pregnant mice were deeply anesthetized with sodium pentobarbitone (Somnopentyl; Kyoritsu Pharmaceuticals) and their uterine horns were exposed. After DNA injection, the head of the embryo inside the uterus was placed between the electrodes (tweezers type, 3 mm diameter; CUY650P3; NEPA GENE, Chiba, Japan) and electroporated using a train of square pulses (50–60 ms long, either 27, 36 or 45 V) repeated four times at an interval of approximately 1 s. After electroporation, embryos were allowed to develop normally until they were sacrificed. In some cases, pups were delivered normally and sacrificed afterwards (see results).

Current measurements

The current was estimated by placing a small resistor (1 Ω) in series with the electroporation electrodes. The voltage drop *V* across this resistor was measured using a digital storage oscilloscope (InfiniiVision 3024A MSO-X; Agilent technologies), the waveform was saved and the corresponding current *I* was calculated ($I = V/1\ \Omega$).

Imaging

The animals were anesthetized with sodium pentobarbitone (Somnopentyl;Kyoritsu Pharmaceuticals) and fixed by perfusion with 4% paraformaldehyde in phosphate buffered saline, immersed in 30% sucrose, embedded in OCT compound (Miles), coronal sections (20 μm) were cut using a cryostat and mounted onto to SuperFrost Plus glass slides. Sections were washed with PBS (phosphate buffered saline, pH7.4) and counter-stained with 4′6′-diamidino-2-phenylindole dihydrochloride (DAPI). DAPI stained nuclei and native fluorescence of EGFP and DsRed were imaged using a standard fluorescent microscope equipped with the appropriate filter sets. For assessment of electroporation efficiency pictures of whole brains were taken using a stereo fluorescence microscope and the area of GFP fluorescence was measured.

Software for data, statistics, diagrams, figures

Data were organized and stored using Excel and OpenOffice. ImageJ (Schindelin *et al.* 2012) was used for image analysis; R (R Development Core Team 2011; http://www.R-project.org) was used for statistics with the R package lattice (Sarkar 2008; http://r-forge.r-project.org/projects/lattice/) for diagrams. Final figures were arranged using Canvas X (for Mac OS; Deneba Systems, now ACD systems) and Inkscape (The Inkscape Team, version 0.48.2, developmental release 9819, http://www.inkscape.org).

Results

Voltage dependency of electroporation

For testing the electroporator nine consecutive embryos in the left uterine horn of a pregnant mouse were injected with 1 μL of DNA solution containing 1 μg/μL pCAG:EGFP and 0.05% w/v Fast Green in sterile saline (Fig. 2B). After injection of all embryos the first three were electroporated using 45 V (L1–3), the next three with 36 V (L4–6) and the last three with 27 V (L7–9) using tweezers electrodes (Fig. 2C). After 3 days the embryos were collected according to their position in the uterine horn. The fifths embryo (L5) had died, the others were fixed and the brains were dissected and photographed using an epifluorescence microscope with EGFP filter set (Fig. 2D–F). The size of the electroporated area was proportional to the voltage used for electroporation (Fig. 2G). This indicates that the amount of negatively charged DNA transported through the membrane depends linearly on the voltage. But, interestingly, the current flowing through the electrodes on a saline moistened tissue is not constant (Fig. 2H). Electroporation was successful without obvious tissue damage as coronal sections showing numerous migrating neurons in the cortical plate (Fig. 2I). This fully resembled the results when using a commercially available electroporator.

Further applications

Two plasmids, pCAG:EGFP and pCAG:DsRed, were used for electroporation. These vectors efficiently (Niwa *et al.* 1991) drive the expression of green or red fluorescent proteins. Electroporation at E13.5 and E15.5 targets layer IV pyramidal and spiny stellate neurons as well as layer II pyramidal cells, respectively. After birth both EGFP and DsRed fluorescence can be observed through the cranial bone and overlying skin (Fig. 3A,B). The fluorescence is so strong that successfully electroporated pups can be selected within 2 days after birth based on screening using a conventional epifluorescence microscope.

Reversing the polarity of the electrodes and adjusting the tilt, the electrodes can target pyramidal cells of the hippocampus (Fig. 3C,D; see Pacary *et al.* 2012). After injection (Fig. 3E) the electroporation at E14.5 with reversed polarity (Fig. 3F) leads to expression of DsRed in pyramidal cells of the CA1 region, which can be observed at 3 weeks postnatal (Fig. 3G). Actually, after longer diffusion of the injected DNA to the contralateral side (e.g. as in the experiments shown in Fig. 2) often the hippocampus also becomes electroporated when targeting the neocortex.

Discussion

The electroporator was easy to assemble and could be used to efficiently electroporate the developing neocortex of mice.

Usually, the square pulse generators for electroporation consist of a variable high-voltage power supply, a capacitor for energy storage, a fast power MOSFET (metal-oxide-semiconductor field-effect transistor) or IGBT (insulated-gate bipolar transistor) and a triggering circuit (fig. 3 in Puc *et al.*, 2004). Our electroporator

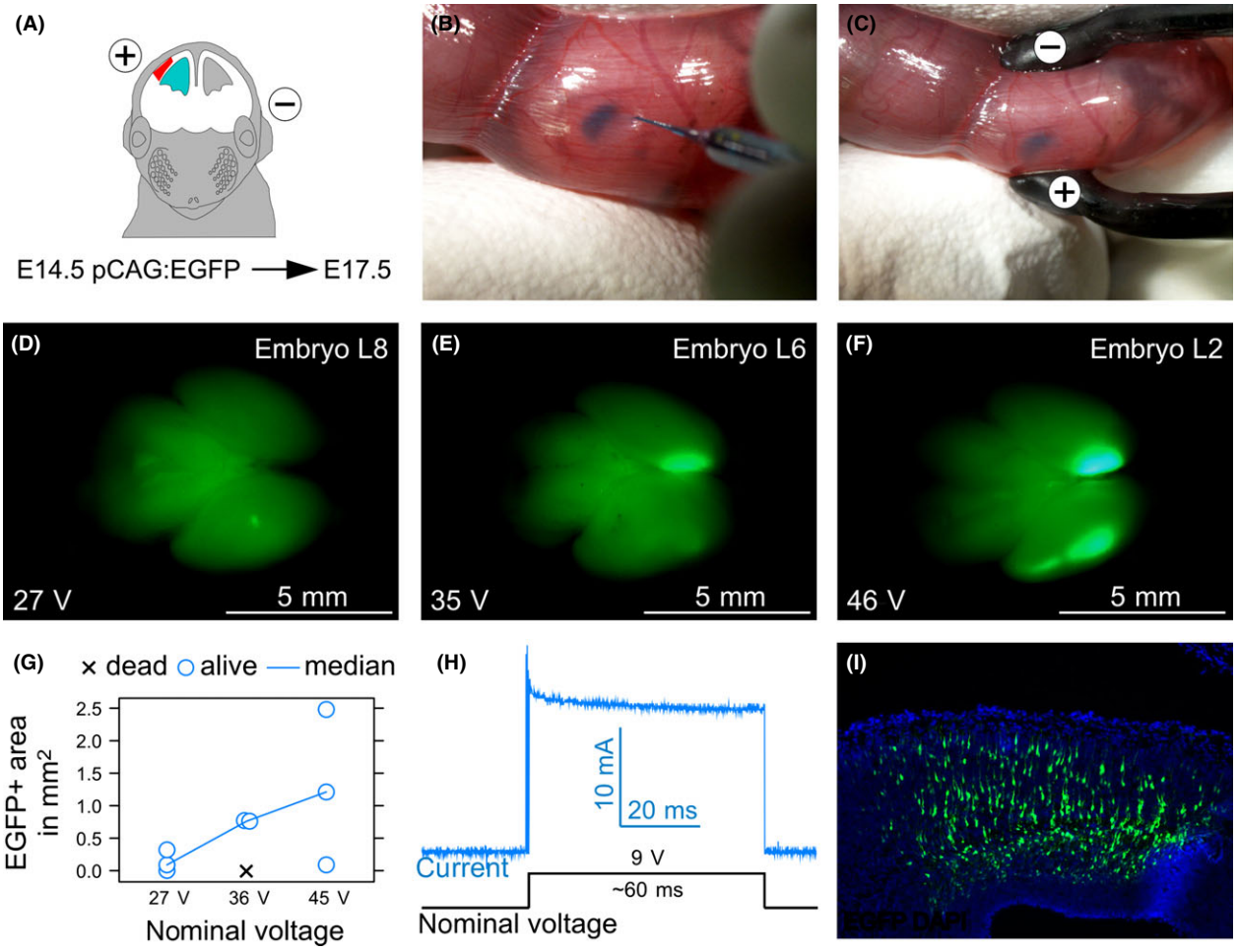

Fig. 2. Electroporation was performed on E14.5 and embryos were harvested on E17.5 (A). Injection of DNA solution into the ventricle can be seen by the addition of vital dye such as Fast Green (B) and this also helps in positioning of the electrodes (C). Examples of the native fluorescence of EGFP in fixed brains observed after electroporation with 27 V (D), 36 V (E), and 45 V (F). The area of electroporation is proportional to the voltage (G). The current through the tweezers' electrodes indicates charging effects on the electrodes and/or the tissue. A coronal section obtained from the brain shown above (F) was counterstained with nuclear marker DAPI (4′6′-diamidino-2-phenylindole dihydrochloride). It shows numerous enhanced green fluorescent protein (EGFP) expressing neurons still migrating within the cortical plate (I).

uses batteries or a variable external power supply and a relay with a simple triggering circuit. The simple triggering circuit allows pulse lengths from 20 to 200 ms with an accuracy of approximately 10%; the foot switch can deliver repeated pulses. The current flow during each pulse shows a sharp rise and an exponential decay towards a plateau phase. This has been previously observed for voltage-controlled electroporation (fig. 3 in De Vry *et al.* 2010) and although this has also been attributed to resistance drops due to pore formation, we think it is most likely due to charging effects on the electrodes. The efficiency of electroporation is proportional to the total charge delivered (Vasilkoski *et al.* 2006; Pucihar *et al.* 2011), hence to pulse duration × voltage × times. Therefore, longer pulses, higher voltage or higher number of pulses are likely to achieve higher electroporation efficiencies. On the other hand, tissue damage increases with higher voltage and therefore increasing the other parameters is more useful. During the pulse, formation of bubbles by electrolysis is seen. Shorter pulses and longer inter-pulse intervals help to prevent formation. Severe tissue damage and damage to the device by accidental short circuit is prevented by the current limiter included in the output circuit, which limits the maximal current through the electrodes to 125 mA. However, in our experience, using standard electroporation conditions, the handling of the embryos causes most of the tissue damage and premature embryo death during the surgery, especially in the earlier stages.

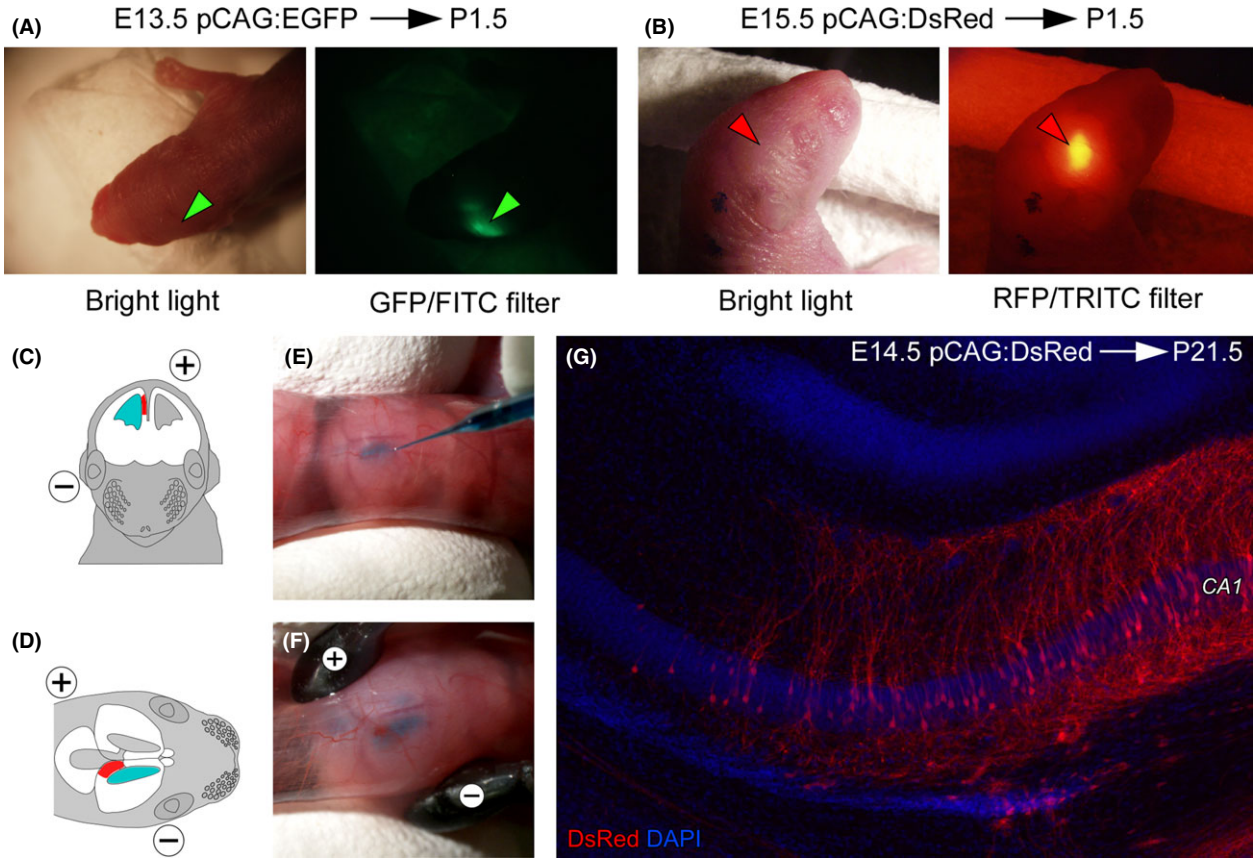

Fig. 3. Further practical applications of electroporation. Shortly after electroporation, the electroporated area in the neocortex can be seen through bone and skin (A, B) using a standard epifluorescence microscope. Electroporation of CA1 pyramidal neurons is achieved by reverse positioning of electrodes (C, D), which directs electroporation to the cortical hem at E14.5, which develops into the hippocampal formation (G). Note that the positive electrode is positioned above the cortex, contralateral to the injection side (E), and tilted both 45° caudal and 45° lateral (F).

In utero electroporation can be used to target different subpopulations of neurons in the developing mouse brain. Principal neurons on different neocortical layers can be targeted by the timing of electroporation, in mice layer II/III at E15.5 and E16.5, IV at E14.5 and E13.5, V/VI at E12.5 and E11.5 and finally the subplate layer at E10.5. By reversing the polarity of electrodes at E14.5 the hippocampus can be electroporated as it has been described before, as well as electroporation of Purkinje cells in the cerebellum (E11.5 according to Nishiyama *et al.* 2012; E14.5 using a triple-electrode, dal Maschio *et al.* 2012) and of interneurons (by targeting the subpallium; Borrell *et al.* 2005).

The efficiency of electroporation depends on the age, region and experience of the experimenter, but usually between 50% and 90% of all embryos show expression of a fluorescent marker protein. Often, not all embryos have been electroporated and whole litters are raised until they reach a certain postnatal age before they are sacrificed and investigated. More efficient is the selection of successful electroporated pups at birth, which is easy in case the neocortex was targeted, because the fluorescence can be observed through the overlaying skull and skin. After birth, expression driven by the pCAG promotor is stable for at least 4 weeks. Later during development DNA is gradually lost from the neurons. A permanent expression could be achieved by integration in the nuclear DNA, using retrotransposons such as Piggyback, TolII and SB11 (Wu *et al.* 2006) or phiC31 integrase (Chalberg *et al.* 2005).

Although the primary purpose for this device is *in utero* and *in ovo* (not shown) electroporation it could also be used for electroporation of DNA into cultured cells (Yamauchi *et al.* 2004) or brain slices (Kawabata *et al.* 2004) and electroporation loading of calcium-sensitive dyes into tissue or single cells (Bonnot *et al.* 2005; Nevian & Helmchen 2007; Hovis *et al.* 2010). *In vivo* electroporation using this device of the postnatal mouse brain (Boutin *et al.* 2008; Fernández *et al.* 2011) is strongly discouraged. This technique requires

higher voltages (100 V), which is above the limit DC voltage of 45 V that is considered harmless to humans. Therefore several safety measures must be included in a electroporator for such applications. We hope that our electroporator will further stimulate the use of electroporation in research (like other free, open-source hardware; Pearce 2012) and in education (like the inexpensive equipment for electrical recording and stimulation; Land *et al.* 2001, 2004).

Acknowledgments

The authors would like to thank Ulrich Bullmann for the help building the electroporator(s), Yuko Gonda and Mayumi Okamoto for the instructions for *in utero* electroporation and providing plasmids. The Foreign Postdoctoral Researcher (FPR) fellowship program at RIKEN supported Torsten Bullmann.

Author's contribution

TB built the equipment, planned, designed, and performed experiments, analyzed the data, wrote the paper. TA designed experiments and discussed the results; UF, CH discussed the results, wrote the paper.

References

Ando, T. & Fujiwara, H. 2013. Electroporation-mediated somatic transgenesis for rapid functional analysis in insects. *Development* **140**, 454–458.

Bonnot, A., Mentis, G. Z., Skoch, J. & O'Donovan, M. J. 2005. Electroporation loading of calcium-sensitive dyes into the CNS. *J. Neurophysiol.* **93**, 1793–1808.

Borrell, V., Yoshimura, Y. & Callaway, E. M. 2005. Targeted gene delivery to telencephalic inhibitory neurons by directional in utero electroporation. *J. Neurosci. Methods* **143**, 151–158.

Boutin, C., Diestel, S., Desoeuvre, A., Tiveron, M. C. & Cremer, H. 2008. Efficient in vivo electroporation of the postnatal rodent forebrain. *PLoS ONE* **3**, e1883.

Chalberg, T. W., Genise, H. L., Vollrath, D. & Calos, M. P. 2005. phiC31 integrase confers genomic integration and long-term transgene expression in rat retina. *Invest. Ophthalmol. Vis. Sci.* **46**, 2140–2146.

De Vry, J., Martínez-Martínez, P., Losen, M., Temel, Y., Steckler, T., Steinbusch, H. W., De Baets, M. H. & Prickaerts, J. 2010. In vivo electroporation of the central nervous system: a non-viral approach for targeted gene delivery. *Prog. Neurobiol.* **92**, 227–244.

Fernández, M. E., Croce, S., Boutin, C., Cremer, H. & Raineteau, O. 2011. Targeted electroporation of defined lateral ventricular walls: a novel and rapid method to study fate specification during postnatal forebrain neurogenesis. *Neural Dev.* **6**, 13.

Fukuchi-Shimogori, T. & Grove, E. A. 2001. Neocortex patterning by the secreted signaling molecule FGF8. *Science*, **294**, 1071–1074.

Gonda, Y., Andrews, W. D., Tabata, H., Namba, T., Parnavelas, J. G., Nakajima, K., Kohsaka, S., Hanashima, C. & Uchino, S. 2013. Robo1 regulates the migration and laminar distribution of upper-layer pyramidal neurons of the cerebral cortex. *Cereb. Cortex* **23**, 1495–1508.

Hovis, K. R., Padmanabhan, K. & Urban, N. N. 2010. A simple method of in vitro electroporation allows visualization, recording, and calcium imaging of local neuronal circuits. *J. Neurosci. Methods* **191**, 1–10.

Kawabata, I., Umeda, T., Yamamoto, K. & Okabe, S. 2004. Electroporation-mediated gene transfer system applied to cultured CNS neurons. *NeuroReport* **15**, 971–975.

Land, B. R., Wyttenbach, R. A. & Johnson, B. R. 2001. Tools for physiology labs: an inexpensive high-performance amplifier and electrode for extracellular recording. *J. Neurosci. Methods* **106**, 47–55.

Land, B. R., Johnson, B. R., Wyttenbach, R. A. & Hoy, R. R. 2004. Tools for physiology labs: inexpensive equipment for physiological stimulation. *J. Undergrad. Neurosci. Educ.* **3**, A30–A35.

LoTurco, J., Manent, J. B. & Sidiqi, F. 2009. New and improved tools for in utero electroporation studies of developing cerebral cortex. *Cereb. Cortex* **19**, i120–i125.

dal Maschio, M., Ghezzi, D., Bony, G., Alabastri, A., Deidda, G., Brondi, M., Sato, S. S., Zaccaria, R. P., Di Fabrizio, E., Ratto, G. M. & Cancedda, L. 2012. High-performance and site-directed in utero electroporation by a triple-electrode probe. *Nat. Commun.* **3**, 960.

Muramatsu, T., Mizutani, Y., Ohmori, Y. & Okumura, J. 1997. Comparison of three nonviral transfection methods for foreign gene expression in early chicken embryos in ovo. *Biochem. Biophys. Res. Commun.* **230**, 376–380.

Nakamura, H. & Funahashi, J. 2013. Electroporation: past, present and future. *Dev. Growth Differ.* **55**, 15–19.

Nevian, T. & Helmchen, F. 2007. Calcium indicator loading of neurons using single-cell electroporation. *Pflugers Arch.* **454**, 675–688.

Nishimura, Y. V., Shinoda, T., Inaguma, Y., Ito, H. & Nagata, K. 2012. Application of in utero electroporation and live imaging in the analyses of neuronal migration during mouse brain development. *Med. Mol. Morphol.* **45**, 1–6.

Nishiyama, J., Hayashi, Y., Nomura, T., Miura, E., Kakegawa, W. & Yuzaki, M. 2012. Selective and regulated gene expression in murine Purkinje cells by in utero electroporation. *Eur. J. Neurosci.* **36**, 2867–2876.

Niwa, H., Yamamura, K. & Miyazaki, J. 1991. Efficient selection for high-expression transfectants with a novel eukaryotic vector. *Gene* **108**, 193–199.

Okamoto, M., Namba, T., Shinoda, T., Kondo, T., Watanabe, T., Inoue, Y., Takeuchi, K., Enomoto, Y., Ota, K., Oda, K., Wada, Y., Sagou, K., Saito, K., Sakakibara, A., Kawaguchi, A., Nakajima, K., Adachi, T., Fujimori, T., Ueda, M., Hayashi, S., Kaibuchi, K. & Miyata, T. 2013. TAG-1-assisted progenitor elongation streamlines nuclear migration to optimize subapical crowding. *Nat. Neurosci.* **16**, 1556–1566.

Pacary, E., Haas, M. A., Wildner, H., Azzarelli, R., Bell, D. M., Abrous, D. N. & Guillemot, F. 2012. Visualization and genetic manipulation of dendrites and spines in the mouse cerebral cortex and hippocampus using in utero electroporation. *J. Vis. Exp.* **65**, 4163.

Pearce, J. M. 2012. Materials science. Building research equipment with free, open-source hardware. *Science* **337**, 1303–1304.

Puc, M., Corović, S., Flisar, K., Petkovsek, M., Nastran, J. & Miklavcic, D. 2004. Techniques of signal generation required for electropermeabilization. Survey of electropermeabilization devices. *Bioelectrochemistry* **64**, 113–124.

Pucihar, G., Krmelj, J., Reberšek, M., Napotnik, T. B. & Miklavčič, D. 2011. Equivalent pulse parameters for electroporation. *IEEE Trans. Biomed. Eng.* **58**, 3279–3288.

R Development Core Team. 2011. R: A language and Environment for Statistical Computing. *R Foundation for Statistical Computing*, Vienna, Austria.

Saito, T. & Nakatsuji, N. 2001. Efficient gene transfer into the embryonic mouse brain using in vivo electroporation. *Dev. Biol.* **240**, 237–246.

Sarkar, D. 2008. *Lattice: Multivariate Data Visualization with R*. Springer, New York, NY.

Schindelin, J., Arganda-Carreras, I., Frise, E., Kaynig, V., Longair, M., Pietzsch, T., Preibisch, S., Rueden, C., Saalfeld, S., Schmid, B., Tinevez, J. Y., White, D. J., Hartenstein, V., Eliceiri, K., Tomancak, P. & Cardona, A. 2012. Fiji: an open-source platform for biological-image analysis. *Nat. Methods* **9**, 676–682.

Sugimoto, T. N. & Tsuchida, T. 2014. Simple electroporation device for gene functional analyses in insects. *Appl. Entomol. Zool.* **2014**, 1–5.

Tabata, H. & Nakajima, K. 2001. Efficient in utero gene transfer system to the developing mouse brain using electroporation: visualization of neuronal migration in the developing cortex. *Neuroscience* **103**, 865–872.

Taniguchi, Y., Young-Pearse, T., Sawa, A. & Kamiya, A. 2012. In utero electroporation as a tool for genetic manipulation in vivo to study psychiatric disorders: from genes to circuits and behaviors. *Neuroscientist* **18**, 169–179.

Vasilkoski, Z., Esser, A. T., Gowrishankar, T. R. & Weaver, J. C. 2006. Membrane electroporation: The absolute rate equation and nanosecond time scale pore creation. *Phys. Rev. E Stat. Nonlin. Soft Matter Phys.* **74**, 021904.

Wu, S. C., Meir, Y. J., Coates, C. J., Handler, A. M., Pelczar, P., Moisyadi, S. & Kaminski, J. M. 2006. piggyBac is a flexible and highly active transposon as compared to sleeping beauty, Tol2, and Mos1 in mammalian cells. *Proc. Natl Acad. Sci. USA* **103**, 15008–15013.

Yamauchi, F., Kato, K. & Iwata, H. 2004. Spatially and temporally controlled gene transfer by electroporation into adherent cells on plasmid DNA-loaded electrodes. *Nucleic Acids Res.* **32**, e187.